Article

Journal of the Brazilian Chemical Society

https://dx.doi.org/10.21577/0103-5053.20240142

J. Braz. Chem. Soc. **2025**, *36*, 2, e-20240142, 1-13
©2025 Sociedade Brasileira de Química

In silico Therapeutic Potential of Phytochemical from *Commiphora leptophloeos* Mart. - J. B. Gillett Leaves Essential Oil against COVID-19

Michel R. R. Souza,[a] Daniela Droppa-Almeida,[b] Helena A. C. Kodel,[a] Tatiane B. Santos,[b] Ashlley S. Moraes,[a] Laiza C. Krause[c] and Thiago R. Bjerk *,[a]

[a]*Laboratório de Cromatografia (LabCrom), Instituto de Tecnologia e Pesquisa (ITP), Universidade Tiradentes (UNIT), 49032-490 Aracaju-SE, Brazil*

[b]*Laboratório de Morfologia e Patologia (LMPE), Instituto de Tecnologia e Pesquisa (ITP), Universidade Tiradentes (UNIT), 49032-490 Aracaju-SE, Brazil*

[c]*Coordenadoria do Curso Integrado em Química, Instituto Federal de Sergipe (IFS), 49055-260 Aracaju-SE, Brazil*

The *in silico* study aimed to suggest phytochemicals from *Commiphora leptophloeos* leaves essential oil as therapies against coronavirus disease (COVID-19) (or severe acute respiratory syndrome coronavirus 2, SARS-CoV-2). For that, we used molecular docking (MD), absorption, distribution, metabolism, excretion, and toxicity (ADMET) parameters, and pharmacokinetic analysis. MD showed the presence of hydrophobic and hydrogen bonds for nine compounds. β-Selinene and bicyclogermacrene showed the best interaction values with the protein Mpro (ID: 6Y2F) (–5.9) and chimeric receptor complexed with its receptor human ACE2 (ID: 6VW1) (–6.1 and –5.5) proteins, as well as low gastrointestinal and high epithelial absorptions, medium permeability for Caco-2 cells and high epithelial permeability, low oral excretion, and were inhibitors of CYP2C19 and CYP2C9 enzymes. On the other hand, both were not permeable to the blood-brain barrier and inhibitors or substrates for glycoprotein-D, and showed carcinogenic potential, but only β-selinene was considered mutagenic. Although little bioavailable, both presented aspects structurally adequate, being compounds with moderate synthesis difficulty. Therefore, more analyses are necessary to evaluate the mechanism of action and unsatisfactory parameters foreseen in bioinformatic assays.

Keywords: SARS-CoV-2, molecular docking, ADMET, bicyclogermacrene, β-selinene

Introduction

On March 11, 2020, the world started a real war against the SARS-CoV-2 (severe acute respiratory syndrome coronavirus 2) virus, popularly called COVID-19 (coronavirus disease). Unfortunately, approximately 770 million cases and 7 million deaths were registered worldwide at the time of writing this paper (September 12, 2023).[1] Therefore, the search for prevention and treatment of the COVID-19 (or SARS-CoV-2) has been intensified by the high mortality rates. Thus, emergency vaccines were authorized to prevent the worsening of the illness, and there is no drug treatment approved.[2] It is worth mentioning that some treatments including bronchodilators, anticoagulants, and anti-inflammatory drugs are used.[3]

The SARS-CoV-2 genome has shown a high frequency of recombination and mutations, demonstrating an illness difficult to treat.[4] Thus, researchers have been looking for new drugs that target the SARS-CoV-2 virus main protease (Mpro or 3CLpro).[2,5,6] Therefore, the use of medicinal plants is one of the oldest therapeutic practices. Often and mainly in poor regions, this practice is one of the few accessible ones, due both to the lack of public health systems and to expensive conventional medical treatments.

The specie *Commiphora leptophloeos* (*C. leptophleos*) Mart. - J. B. Gillett is a native tree found in South America, mainly in Bolivia and Brazil, and is usually known for its medicinal purposes.[7-9] In Sergipe, Brazil, *C. leptophloeos* is a tree that has a high timber value and can be used in civil construction, carpentry, and handicrafts.

The species has been historically used in traditional medicine, mainly derived from indigenous ancestry, as is the case of the Karirishokó and Shokó tribes, from Alagoas

*e-mail: thiagobjerk@gmail.com
Editor handled this article: Paula Homem-de-Mello (Associate)

This is an open-access article distributed under the terms of the Creative Commons Attribution License.

and Sergipe states, Brazil.[10] Its use as a medicinal plant is done through the development of syrups, infusions, incense, and extraction of medicinal oils, using the bark of the stem, seed, leaves, flower, and the wood of the tree, for the treatment of diseases, such as infectious, pains, nausea, diarrhea, diabetes, and urinary tract inflammation.[7,10] For example, the decoction of a handful of stem bark in a liter of water and made with sugar as a syrup (a spoonful is drunk 5-6 times a day) in the flu treatments, coughs, and bronchitis; or leave soaking to drink in treatment of influenza and stomachache healing.[11,12]

The chemical composition of this species is little known, presenting sesquiterpenes and monoterpenes in the leaf essential oil, as well as phenolic compounds, flavonoids, reducing sugars, tannins, coumarins, saponins, alkaloids, albumins, terpenes, and steroids in the extract of barks and leaves.[7-10,13-16] In this sense, *in silico* works suggest phytochemicals such as promising therapies against SARS-CoV-2.[3,4,17,18]

Therefore, this study aims to suggest new phytochemicals such as therapies against SARS-CoV-2. Thus, the essential oil compounds from *C. leptophloeos* leaves were separated and identified by gas chromatography-mass spectrometry, respectively. We have achieved an *in silico* study using molecular docking analysis. Besides that, we propose a bioeconomic development of this plant, which would avoid deforestation.

Experimental

Sample collection

C. leptophloeos leaves were collected in 2019 (September 14; winter) in Poço Redondo-SE (9°48'25.6"S 37°38'12.9"W), Northeast Brazil. The register of the collection was ICMBio MMA number 70804-1. The leaves were packed in kraft paper bags. In the laboratory, were cleaned with distilled water and dried (40 °C for 48 h) in an oven. Soon after, crushed in a steel knife mill, sifted (32-60 mesh), and stored in glass jars (hermetically sealed).

Materials

The solvent dichloromethane (DCM) was obtained from Synth (Diadema, Brazil). Anhydrous sodium sulfate (calcined to 500 °C for 4 h) was obtained from Neon (Suzano, Brazil). Certificated standards of linear *n*-alkanes (*n*-C8 to *n*-C40 + pristane and phytane: 500 μg mL^{-1}, in DCM) were purchased from Sigma-Aldrich (St. Louis, USA).

Essential oil extraction

The extraction of essential oil from *C. leptophloeos* leaves was performed by hydrodistillation type Clevenger using 127 g, crushed in 2 L of deionized water at a temperature of 100 °C for 4 h. Soon after, the oil was collected, dried in anhydrous sodium sulfate column, and stored in vials, protected from the light. For chromatographic analyses, 0.01 g of essential oils (separately) were weighed and diluted into DCM to a final volume of 1 mL.

Chromatographic conditions

All chromatographic analyses were performed using a GC-MS (gas chromatography-mass spectrometry) (model GCMS-QP2010 plus from Shimadzu, Kyoto, Japan) and electron ionization (EI, 70 eV) mode, equipped with an automatic injector (model AOC-20i from Shimadzu, Kyoto, Japan). It used a ZB-5 column from Zebron (5% phenyl 95% dimethylpolysiloxane; 30 m, 0.25 mm internal diameter (ID), and 0.25 μm film thickness) (Torrance, USA). The oven temperature program was: 60.0 °C (hold 0.0 min), ramp to 200.0 °C at 2.0 °C min^{-1}, ramp to 300.0 °C at 10.0 °C min^{-1} (hold 16.0 min). The temperatures of the injector, interface, and ionization source were 220.0, 300.0, and 280.0 °C, respectively. The helium gas flow (99.9995%) was 0.8 mL min^{-1}. The injection (1 μL) was conducted in split mode (1:50).

Data treatment was achieved using the software GC-MS solution (version 2.6.1), with a signal/noise ratio higher than or equal to 3. In this sense, a hydrocarbon standard mixture (C8 to C40) was injected under the same conditions as the samples and according to the equation developed by Dool and Kratz.[19] Thus, the linear temperature programmed retention index (LTPRI) was determined. The mass spectrum of each compound and LTPRI obtained experimentally were compared (tentative method) with those available in the NIST (National Institute of Standards and Technology) web library, for a ZB-5 column or similar, as well as with the Adams database.[20] Compounds that showed a difference of up to 20 units concerning the theoretical retention index and whose spectrum similarity was greater than 80% were considered identified. The compounds with an area above 3% were selected for the *in silico* step. Thus, PubChem was accessed to obtain their canonical SMILES (simplified molecular input line entry system) and their three-dimensional structures.[21]

Molecular docking

For molecular docking, the previously selected

compounds and their three-dimensional structures obtained by PubChem served as ligands for the prediction of interaction with protein Mpro (ID: 6Y2F) and chimeric receptor complexed with its receptor human ACE2 (ID: 6VW1*)* both obtained from the Protein Data Bank (PDB) and described as molecular targets important for SARS-CoV-2.[21,22]

The protein complexes, along with their corresponding receptors, underwent modifications to isolate the proteins. This was done by eliminating water molecules, ions, and bound receptors from the complexes. These modifications were implemented to refine the system for subsequent molecular docking simulations, aiming to enhance accuracy and specificity in ligand binding interactions. Molecular docking was performed using AutoDock Vina 4 and the analysis and visualization of interactions were performed using the Biovia Discovery Studio Visualizer.[23,24] The present study employed a specific docking method, using a grid box approach. For the spike protein, the coordinates used were as follows: center_x = 87.568000, center_y = 42.411000, center_z = 99.745000, with dimensions of size_x = 50, size_y = 50, size_z = 50, and an exhaustiveness value of 8. Similarly, for the M protein, the coordinates utilized were: center_x = –88.338585, center_y = –26.319946, center_z = 87.765713, with dimensions of size_x = 40, size_y = 40, size_z = 40, and an exhaustiveness value of 8. The grid box dimensions were acquired from the Protein Data Bank (PDB)[22] using the Discovery Studio tool.[24]

To enhance the validation of molecular docking interactions between spike protein, M protein and the compounds β-selinene and bicyclogermacrene, the study also utilized DockThor-VS, a free web server renowned for protein-ligand docking.[25] Consistent with our method, DockThor-VS was configured with identical grid box parameters as previously described but distinguished itself by conducting up to 24 runs. It is noteworthy that only the top-ranking results derived from the affinity analysis conducted by Discovery Studio were selected for later validation utilizing DockThor-VS.[25]

Pharmacokinetic analysis

The pharmacokinetic analysis took place in two stages, using two online software. The first software was SwissADME,[26] which predicted the gastrointestinal absorption, the permeability of the blood-brain barrier (BBB), the substrates, and inhibition of P-glycoprotein, the cytochrome P-450 inhibitors CYP2C19, CYP2C9, CYP2D6, and CYP3A4, as well as, of skin permeation. The second software was PreADMET and Prediction of ADME/Tox,[27] which performed both the pharmacokinetic analysis step and the toxicity analysis. In the pharmacokinetic analysis phase, to complement the information collected by SwissADME, PreADMET, Prediction of ADME/Tox predicted CYP2D6 substrate and CYP3A4 substrate, as well as MDCK Cell Permeability.

For the ADMET analysis, it was necessary to use canonical SMILES. For the analysis of the toxicity of the compounds, it was also predicted using the PreADMET and Prediction of ADME/Tox[27] to verify acute algal toxicity, Ames test, carcinogenicity (mouse), carcinogenicity (rat), acute daphine toxicity, *in vitro* human ether-related gene (hERG) inhibition, acute fish toxicity (medaka), acute toxicity in fish (minnow), Ames TA100 (+S9), Ames TA100 (–S9), Ames TA1535 (+S9) and Ames TA1535 (–S9). With this same software, it was possible to verify the drug-likeness option that analyzes the rule of five or Lipinski's rule as it is also known, associated with the lead rule, CMC similarity rule, MDDR-type rules, reactive functional group, and rule WDI type.

Results and Discussion

Essential oil chemical characterization

The hydrodistillation of *C. leptophloeos* leaves produced 0.0004% of essential oil, considered low to the yield determined by Silva *et al*.,[13] (0.08%) and Pinto *et al*.,[14] (2.05%). Nevertheless, this essential oil was characterized and presented 139 compounds, of which 119 were identified in 99.95% of the total oil (Table S1 and Figure S1, presented in the Supplementary Information (SI) section).

Major compound classes showed sesquiterpene (61.28%), oxygenated sesquiterpenes (28.69%), and oxygenated diterpenes (4.33%). Monoterpenes and oxygenated monoterpenes presented 0.42 and 0.12%, respectively, while 3.90% of compounds were not identified. Other compounds, representing chemical classes such as *n*-alkanes, fatty acid methyl ester (FAMEs), esters, and ketones were determined in the proportion of 1.21%. Silva *et al*.,[13] also presented sesquiterpene as the majority with 46.4%.

However, different from this study, the monoterpene class was the second majority (43.4%), followed by oxygenated sesquiterpenes (6.2%). Therefore, the leaf essential oil was composed almost exclusively of terpenoids C15, in which sesquiterpenes constituted the main components. Shen *et al*.,[28] showed a compositional variety in different species of *Commiphora*, being predominant in the sesquiterpenoids with a low degree of oxidation. Sesquiterpenes are derived from farnesyl diphosphate and

present an elevated level of biological activities, as well as ecological roles for the interaction between plant-pathogen, pollinator attraction, and plant-insect.[29]

The compounds identified by chromatography present in the oil obtained from *C. leptophloeos* leaves and with a percentage area above 3% were a total of nine compounds (Figure 1). Of these, only one was classified as a diterpene and the others were considered sesquiterpenes.

Individually, the main compounds (area > 3%) shown in the leaf essential oil were germacrene B (12.29%) and germacrone (12.24%), followed by β-caryophyllene (8.29%), bicyclogermacrene (6.37%), γ-elemene (5.58%), spathulenol (5.32%), germacrene D (4.6%), phytol (4.18%), and β-selinene (3,23%) (Tables S1 and S2, SI section).

The germacrene group is a main sesquiterpenoid structure determined into the *Commiphora* genus, as reported in the literature.[28] Besides that, the compounds β-elemene, α-copaene, α-humulene, β-selinene, and germacrene B were determined in this work, as well as in different species of *Commiphora*.[28]

The presence of α-phellandrene (26.3%), β-caryophyllene (18%), β-phellandrene (12.9%), germacrene-D (6%), and α-humulene (5.5%) in the *C. leptophloeos* leaves essential oil extracted by Silva *et al.*,[13] is probably due to different regions of plant collection, environmental conditions, genetic variability, and pathophysiological characteristics, which influence the composition of secondary metabolites in plants.[30]

To understand its role in the antiviral activity, a search was conducted on its potential pharmacological activities already described (Table 1).

Molecular docking data

Molecular docking was performed, and the results are recorded in Table 1. The most negative binding energy (EB) is related to the best docking score.[51] Hydrogen bonds are a primary contributing factor in supporting the binding affinity of ligands for the receptor. The strong interaction of the hydrogen bond stands for a high binding capacity between the ligand and the protein.[52] All nine ligands were explicitly embedded in selected receptors. Table 1 revealed that the binding affinity of our ligands with the protein Mpro receptor ranged from –6.1 to –3.9 kcal mol^{-1}, while with the chimeric SARS-CoV-2 receptor complexed with its human ACE2 receptor, it was possible to identify a variation in the binding affinity of this receptor with the ligands between –6.1 to –4.1 kcal mol^{-1}. The best result according to binding energy was to the compound bicyclogermacrene with protein Mpro, presenting –6.1 kcal mol^{-1}, while to the chimeric SARS-CoV-2 receptor complexed with its human ACE2 receptor both germacrene D and β-selinene present binding energies more negative, –6 and –6.1 kcal mol^{-1}, respectively. According to Shityakov *et al.*,[53] interactions below –6 kcal mol^{-1} are more likely to occur spontaneously.

When analyzing the interactions between each compound and its receptors, it can be verified that phytol (Figure S2, SI section) presented only one hydrogen bond with HIS163 present in the active site of protein Mpro with a distance of 2.35 Å, this being considered a type of strong bond, while with the chimeric SARS-CoV-2 receptor complexed with its human ACE2 receptor two hydrogen bonds were identified with ARG439 with distances of 2.40 and 2.75 Å classified as moderate. Both hydrogen

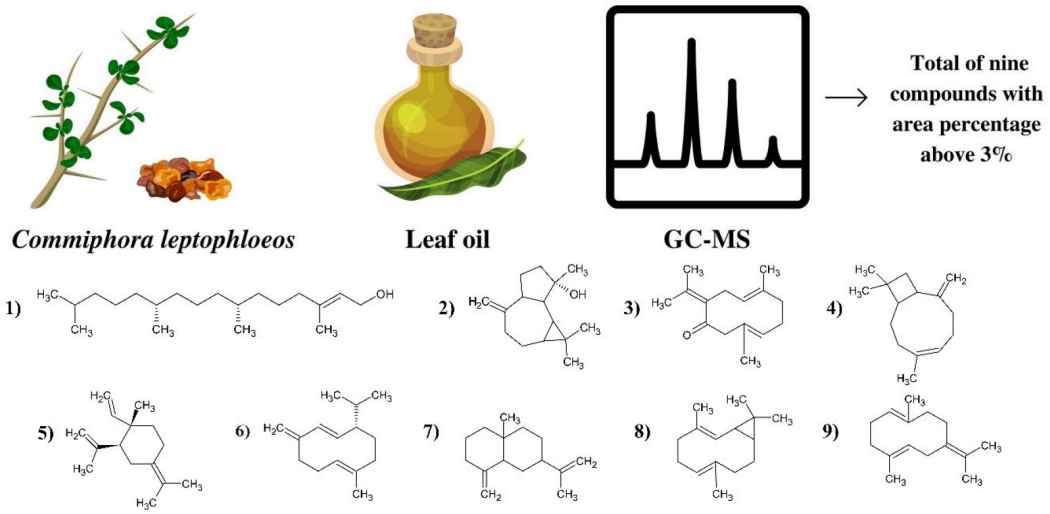

Figure 1. Illustrative image corresponding to the plant used *Commiphora leptophloeos* followed by obtaining the oil from its leaves with subsequent analysis by gas chromatography-mass spectrometry (CG-MS). A total of nine compounds with a percentage area above 3% were identified and selected for *in silico* analysis. (1) Phytol; (2) spathulenol; (3) germacrone; (4) β-caryophyllene; (5) γ-elemene; (6) germacrene D; (7) β-selinene; (8) bicyclogermacrene; and (9) germacrene B.

Table 1. Main compounds obtained through the chromatographic analysis of the essential oil of the leaves of *C. leptophloeos* and their identifications in PubChem. Binding affinity and coupled structures of the nine compounds identified with selected SARS-CoV-2 M protein and spike receptors, and their antiviral activities are already described in the literature

Compound	Classification	PubChem[21] ID	Area > 3%	Binding affinity / (kcal mol^{-1})				PubMed[31]
				M Protein		Spike		
				AutoDock Vina 4[23]	Dockthor-VS[25]	AutoDock Vina 4[23]	Dockthor-VS[25]	
Phytol	diterpene	5280435	4.18	–3.9		–4.1		anti-TMV[32]
Spathulenol	sesquiterpene	92231	5.32	–5.4	–	–5.7	–	anti-HSV-1[33,34]
Germacrone	sesquiterpene	6436348	12.24	–5.2	–	–5.6	–	against porcine reproductive respiratory syndrome, pseudorabies virus, influenza virus, porcine parvovirus, H1N1, and *Calicivirus feline*[35-40]
β-Caryophyllene	sesquiterpene	50064392	8.29	–5.8	–	–5.8	–	against Newcastle disease virus, HSV-1, coronavirus, cucumber mosaic, herpes virus, adenovirus, and hepatitis virus[41-47]
γ-Elemene	sesquiterpene	319332888	5.58	–5.2	–	–5.4	–	–
Germacrene D	sesquiterpene	9548705	4.6	–5.9	–	–6	–	against H1N1 and HSV-1[48-50]
β-Selinene	sesquiterpene	442393	3.23	–5.9	–7.0	–6.1	–7.5	–
Bicyclogermacrene	sesquiterpene	13894537	6.37	–5.9	–6.8	–5.5	–7.2	anti-HSV-1[42]
Germacrene B	sesquiterpene	5281519	12.29	–6.1	–	–5.4	–	–

SARS-CoV-2: severe acute respiratory syndrome coronavirus 2; ID: identification; TMV: tobacco mosaic virus; HSV-1: herpes simplex virus type 1; H1N1: influenza A virus subtype.

interactions occurred due to the presence of the hydroxyl group in phytol.

Following the analysis of the other ligands, spathulenol (Figure S3, SI section) presented two hydrogen bonds, one with GLN192 at 2.37 Å, another with THR190 at 3.36 Å, and a carbon-hydrogen interaction with GLN189 at 2.25 Å, present in the active site of the Mpro protein. To the chimeric SARS-CoV-2 receptor complexed with its human ACE2 receptor, only one hydrophobic interaction of the pi-sigma type was identified with PHE373 at 3.62 Å away. Hydrophobic interactions are quite common because the active sites of proteins commonly present hydrophobic characteristics and, in this case, PHE373 interacted with spathulenol through its aromatic ring present.

Regarding germacrone (Figure S4, SI section) with Mpro protein, only one hydrogen bond was identified between the oxygen present in germacrone and THR199 with a distance of 2.02 Å, considered strong. While with the chimeric SARS-CoV-2 receptor complexed with its human ACE2 receptor, the same oxygen interacted with GLY404 forming hydrogen bonds with 3.16 Å, being considered moderate. Another interaction was also found through a carbon interacting with TYR508 by a hydrophobic pi-sigma bond with 3.66 Å.

On the other hand, β-caryophyllene (Figures S5A and S5B, SI section) with Mpro protein showed only one hydrophobic bond with PHE294, also of the pi-sigma type, with a distance of 3.42 Å. This compound showed two hydrophobic bonds with PHE373 also of the pi-sigma type with distances of 3.77 and 3.79 Å. Related to γ-elemene (Figure S5C, SI section) this compound did not show any interaction at the active site of the Mpro protein of SARS-CoV-2 however, with the spike protein this compound showed a hydrophobic interaction with the PHE373 residue with a distance of 3.78 Å of the pi-sigma type.

Germacrene D (Figures S6A and S6B, SI section) with Mpro protein showed only a hydrophobic bond with PHE294 also of the pi-sigma type with distance of 3.85 Å. This compound also showed two hydrophobic bonds with TRP436 of the pi-sigma type with distances 3.37 and 3.89 Å with chimeric SARS-CoV-2 receptor complexed with its human ACE2 receptor. When analyzing germacrene B (Figures S6C and S6D, SI section) with Mpro protein, it showed two hydrophobic bonds with PHE294, also of the pi-sigma type, with distances of 3.83 and 3.93 Å. Two hydrophobic bonds with PHE490 of the pi-sigma type with distances of 3.69 and 4.00 Å were seen for chimeric

SARS-CoV-2 receptor complexed with its human ACE2 receptor. The similarities between the interactions were already predicted because they are isomeric structures.

When looking at Table 1, the compounds that presented the highest binding energies were bicyclogermacrene for Mpro protein presenting a variety of binding energies between –6.1 to –4.7 kcal mol^{-1}, and chimeric SARS-CoV-2 receptor complexed with its human ACE2 receptor was β-selinene presenting a variety of binding energies between –6.1 to –4.8 kcal mol^{-1}. Both showed hydrophobic interactions (Figure S7, SI section).

But when analyzing the interactions (Figure S8, SI section), starting with β-selinene and Mpro protein, the compound showed a pi-sigma hydrophobic interaction with PHE294 with a distance of 3.48 Å, the same can be observed with the chimeric SARS-CoV-2 receptor complexed with its human ACE2 receptor which also showed a hydrophobic pi-sigma interaction with PHE379 at a distance of 3.59 Å. Regarding the analysis with bicyclogermacrene, hydrophobic pi-sigma bonds were also observed with both proteins. With Mpro protein, the interaction was with PHE294 at 3.51 Å, and with chimeric SARS-CoV-2 receptor complexed with its human ACE2 receptor, it was with residue TYR508 at 3.73 Å.

To understand or design drugs or compounds that have a certain pharmacological activity, the knowledge of protein-ligand binding mechanisms, as well as structural data to explore this potential is of paramount importance. Therefore, a broad understanding of the nature of molecular interaction/recognition is also of immense value, which will provide insights into drug design, development, and discovery. In this context, molecular docking is a widely used computational tool capable of predicting different forms of binding in the protein-ligand interaction. In the present study, molecular docking aimed to predict whether the compounds present in the oil of *C. leptophloeos* leaves and their interaction with important receptors of SARS-CoV-2. For this, molecular docking was done through the adoption of a grid-based technique such as the AutoDock Vina 4.[23] In the dockings performed, hydrogen interactions were predicted, which are considered the strongest among the intermolecular interactions and were classified between strong and moderate. The most present interactions were hydrophobic, which is also quite common between drugs and the site of interaction as this type of interaction ends up increasing the local entropy and benefiting the interaction, indicating the importance of other types of intermolecular interactions that are often called weaker.[54,55]

To confirm the obtained results, the DockThor-VS tool was employed for the top-performing outcomes from the molecular docking conducted by AutoDock Vina 4.[23,25] Although the same sites were used, the compounds showed interactions with distinct amino acid residues. Alkyl hydrophobic interactions prevailed in the analysis, wherein M protein showed interaction with LEU293 and ILE95 residues with the respective distances of 4.53 and 5.37 Å. Furthermore, regarding the interaction of M protein with bicyclogermacrene, it displayed interaction with ILE95 and LEU93 residues, with the respective distances of 4.13 and 4.06 Å. For the spike protein, β-selinene interacted with TYR175, LYS73, and TYR165, measuring distances of 5.20, 4.93, and 5.24 Å. Bicyclogermacrene interaction with spike protein occurred with TYR165 at 4.76 Å, and the two interactions with TYR119 were measured at distances of 4.88 and 5.26 Å.

The use of two software tools has been widely encouraged to verify whether the specifically selected site indeed interacts with the compounds. Even though the interactions involve different amino acid residues, using different tools confirms the prediction. In this case, the residues differed, yet all compose the specific interaction site for each protein and show hydrophobic interactions, common in pockets composed of hydrophobic amino acids.

Both tools are often employed for molecular docking between protein-ligand pairs. AutoDock Vina 4, for instance, was evaluated against a virtual screening benchmark called the Directory of Useful Decoys by the Watowich group and is regarded as one of the most utilized programs in the scientific community due to its agility and high prediction accuracy.[23] Conversely, DockThor-VS is a grid-based method designed for flexible ligand and rigid receptor docking.[25] Affinity prediction and protein-ligand complex classification are performed using the DockTScore linear empirical scoring function.

Pharmacokinetic and physicochemical properties

Among the results found via molecular docking of the nine compounds identified in the oil of *C. leptophloeos* leaves, only two went to the pharmacokinetic, physicochemical, toxicity, and drug-likeness analysis stages (Figure 2).

After verifying the possibility of interaction with important molecular targets of SARS-CoV-2, the two molecular structures β-selinene and bicyclogermacrene were evaluated according to different parameters, to identify those with the best chance of becoming an effective drug for COVID-19. In addition to molecules needing to present high biological activity, they must present low toxicity. Equally important is access and concentration on the therapeutic target in the body. The traditional way of considering pharmacokinetics (i.e., the fate of a therapeutic

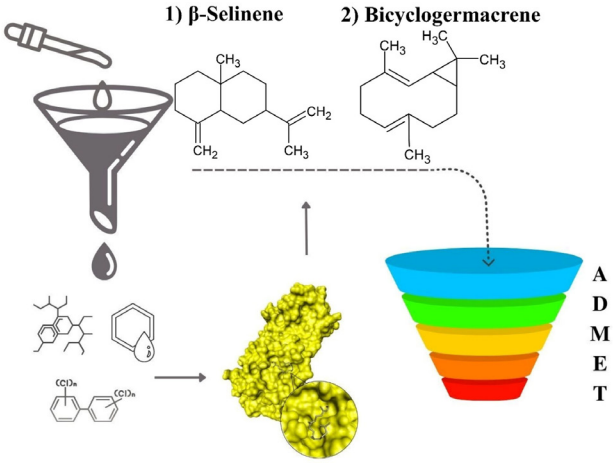

Figure 2. Illustration of compounds that will follow the ADMET (absorption, distribution, metabolism, excretion, and toxicity) steps: (1) β-selinene; (2) bicyclogermacrene.

compound in the body) is to break down the various effects that affect target access into individual parameters. In turn, these ADME parameters (for absorption, distribution, metabolism, and excretion) can be evaluated separately, and considering this, early estimation of ADME in the discovery phase has been shown to dramatically reduce the fraction of pharmacokinetic-related failures in the clinical phases.

Therefore, both previously selected molecules were analyzed by SwissADME[26] and one of the first parameters analyzed is related to their chemical structure arranged in a bioavailability radar, which is a quick analysis to verify the similarity between the added structure and drugs already existing. Figure 3 shows the bioavailability radars of β-selinene and bicyclogermacrene.

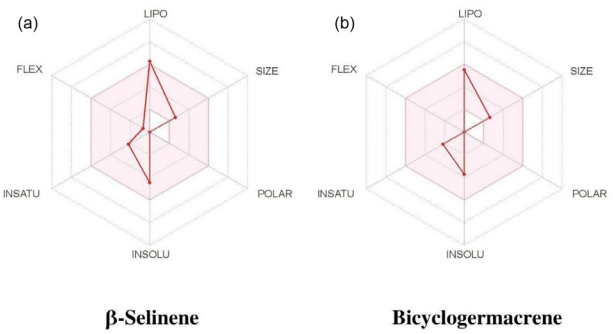

Figure 3. Bioavailability radar of β-selinene, bicyclogermacrene with other drugs already described. The pink area is the ideal range for each analyzed property, lipophilicity, size, polarity, solubility, flexibility, and saturation.

Six physicochemical properties were considered: lipophilicity, size, polarity, solubility, flexibility, and saturation. In this sense, the pink area represents the ideal range for each property mentioned, and the data are described in Table 2.

Table 2. Characteristics of compounds β-selinene and bicyclogermacrene on the availability radar

Characteristic/parameter	β-Selinene	Bicyclogermacrene
Lipophilicity (–0.7 < XLOGP3 < +5)	5.44	4.14
(150 < MW < 500) / (g mol^{-1})	204.35	204.35
Polarity (20 < TPSA < 130) / Å^2	0.00	0.00
Insolubility (0 < logS (ESOL) < 6)	–4.47 moderate	–3.72 soluble
Unsaturation (0.25 < fraction C sp3 < 1)	0.73	0.73
Flexibility (0 < number of rotatable bonds < 9)	1	0

Å: Angstrom; MW: molecular weight; TPSA: topological polar surface area; ESOL: estimated solubility, log S: logarithm of the solubility in water (S); LOGP3: logarithm of partition coefficient (log P).

When analyzing the parameters, the results, and the area, it is clear that the compounds in question are within the drug standards already described in the literature, except for polarity, both are far below the standard stipulated by the algorithm, which analyzes the topology and the surface area.[53] Related to lipophilicity, which is the most important property of a possible drug, as it is related to its absorption, distribution, potency, and elimination capacity, it was noticed in this context that only bicyclogermacrene is within the parameter stipulated by XLOGP3. However, SwissADME presents six different methods to verify the lipophilicity of compounds and even the one developed by SwissADME itself ilogP has been reported[26] as the best predictor for this characteristic. In this context, β-selinene presented 3.28 while bicyclogermacrene presented 3.34.

The parameters on the solubility indicate certain ease in the manipulation of this compound, providing important information, in this case, β-selinene was moderately soluble by the ESOL method and soluble by SILICOS-IT method, which is a linear correlation coefficient of this corrected by the molecular weight is $R^2 = 0.75$, however, it is worth noting that all methods are the decimal logarithm of the molar solubility of water. When talking about bicyclogermacrene, this compound showed solubility in the three methods provided by SwissADME.[26]

When analyzing the pharmacokinetics, Table 3 provides information regarding the two softwares used, SwissADME[26] and PreADMET.[27]

The prediction of pharmacokinetics, i.e., absorption, distribution, metabolism, excretion, toxicity (ADMET), and drug similarity of candidate molecules was performed using the online software SwissADME[26] and PreADMET,[27] tools that are gaining ground for drug discovery today.[56-60] These analyses help in the virtual screening of compounds,

directing the ideal ones, within the parameters established by each tool, to proceed to the search for new drugs.

The results obtained are shown in Table 3.

As depicted in the Table 3, the compounds exhibited low human intestinal absorption, in the analysis provided by PreADMET software.[27] This software uses the brain or intestinal estimated permeation method (BOILED-Egg) to estimate gastrointestinal absorption. The predictive model calculates the lipophilicity and polarity of the compounds, providing estimations for both brain and intestinal permeation. This information is crucial for assessing the viability of oral administration for these compounds, given that orally prescribed drugs must traverse the digestive barrier of the system to reach the bloodstream. Consequently, pharmaceutical laboratories must develop medications that show absorption tailored to the specific pathology of the individual, ensuring optimal medication levels in the bloodstream without excess or deficiency.[60]

The distribution of each compound in the human body depends on factors such as the permeability of the blood-brain barrier (BBB), and in this case, all compounds evaluated in this work, described in Table 3, were negative

Table 3. Tabulated ADMET and drug-likeness properties obtained from SwissADME[26] and PreADMET[27]

Characteristic	Parameter	β-Selinene	Bicyclogermacrene
GI absorption	–	low	low
Caco2	–	23.4924	23.6334
BBB permeant	–	no	no
Pgp substrate	–	no	no
Pgp_inhibition	–	inhibitor	inhibitor
CYP1A2 inhibitor	–	no	no
CYP2C19 inhibitor	–	yes	yes
CYP2C9 inhibitor	–	yes	yes
CYP2D6 inhibitor	–	no	no
CYP_2D6_substrate	–	non	non
CYP3A4 inhibitor	–	no	no
CYP_3A4_substrate	–	substrate	substrate
MDCK	–	57.2175	55.1386
Skin permeability	–	–0.642453	–0.715374
Toxicity	algae_at	0.0134954	0.0131925
	Ames_test	mutagen	non-mutagen
	carcino_mouse	negative	positive
	carcino_rat	positive	positive
	hERG_inhibition	medium_risk	medium_risk
	TA100_10RLI	negative	negative
	TA100_NA	negative	negative
	TA1535_10RLI	negative	negative
	TA1535_NA	negative	negative
Drug-likeness	Lipinski violations	1	1
	Ghose violations	0	0
	Veber violations	0	0
	Egan violations	0	0
	Muegge violations	2	1
	bioavailability score	0.55	0.55
	PAINS alerts	0	0
	Brenk alerts	1	1
	leadlikeness violations	2	2
	synthetic accessibility	3.42	4.34

ADMET: absorption, distribution, metabolism, excretion, and toxicity; GI: gastrointestinal; Pgp: P-glycoprotein; BBB: blood-brain barrier; PAINS: pan-assay interference compounds; MDCK: Madin-Darby canine kidney; hERG: human ether-related gene.

for permeability at BBB. This type of analysis provides important information, as BBB permeability indicates compounds with potential action on the central nervous system (CNS), thus, *in silico* BBB tests are relevant tools to help predict the brain absorption of drug candidates before *in vivo* studies.[61] Once present in the body, the compounds are distributed and can be absorbed by the BBB, which measures the ability of a substance to cross this barrier, however, by the parameters observed, all compounds showed negative results in permeating the BBB and therefore, they are not compounds that act directly on CNS.

Another parameter provided by the tool to evaluate this intestinal permeability is the permeability in epithelial cells, including the Caco-2 intestinal cell lines (intestinal epithelium), originating from human colon adenocarcinoma (large intestine) that can differentiate in enterocytes. According to pharmacokinetic studies,[62,63] the following classification regarding permeability in Caco2 cells is recommended; > 70 nm sec^{-1}: high permeability, 4-70 nm sec^{-1}: medium permeability, > 4 nm sec^{-1}: low permeability, as observed in Table 3 following this model used, the two compounds showed medium permeability to Caco-2 cells. Since PreADMET also predicts skin permeability, it was analyzed as it is an important parameter for the pharmaceutical industry when it correlates with substances that are administered transdermally, as well as for hazard analysis that these substances can cause when coming into contact with the skin of the individual. As a result, these pharmacokinetic analyses were determined according to the classification of skin permeability into low and high, according to studies,[63,64] and the result is provided as high for values < 0.1 and low for values > 0.1, in the effect of these values, it was observed that both analyzed compounds showed high permeability since they showed results < 0.1 for skin permeability.

The other cell type that checks the excretion pathway is the Madin-Darby canine kidney (MDCK), originating from the canine kidney and undergoing differentiation into columnar epithelial cells with semipermeable membranes when cultured.[62,64,65] This MDCK model, as said, measures the rate elimination of drugs, that is, this cell simulates the intestinal epithelial barrier and the property of renal clearance, thus predicting the permeability and excretion of the compound. According to the values obtained, it is seen that there was an enormous variation in these results among the compounds studied. Within this context, it is known that the higher the value presented, the greater the excretion capacity of this compound.[66] Thus, it was observed that both β-selinene and bicyclogermacrene present low excretion by this route, these data were compared with the data of the drug simvastatin.[60]

Still focusing on metabolism and excretion, most drugs depend on factors, such as P-glycoprotein (Pgp), one of the most important cell surface proteins involved in xenobiotic efflux, that is, pumping xenobiotics from the inside to the outside of the cell. Following this same context, another important observation of the result is that the compounds are not substrates but are inhibitors of Pgp. A non-substrate means that Pgp would not recognize the molecule and would not cause its efflux. Being an inhibitor, these molecules prevent or reduce the efflux of drugs from cells, which could cause an increase in the bioavailability of these compounds, potentially enhancing their therapeutic effect. This can be beneficial in cases where Pgp-mediated drug efflux limits the effectiveness of a medication. Nonetheless, inhibition of Pgp-mediated can also lead to increased drug toxicity or adverse effects, as higher drug concentrations may accumulate in tissues.[67,68]

As for the effect on metabolism, one of the most important parameters in the drug development stage is the enzymatic inhibition capacity that a given molecule has. The CYP-450 enzyme complex called cytochrome P450 enzymes (hemeproteins located in the liver), have subfamilies responsible for the drug metabolism process. CYP3A4, CYP2C19, CYP2C9, and CYP2D6 stand out, which are one of the main responsible for the process of drug metabolism. In this context, it was possible to predict that both were able to inhibit the action of CYP2C19 and CYP2C9, but in the other enzymes, the compounds were neither inhibitors nor substrates.

Related to toxicity, PreADMET software[27] is an essential tool for predicting the safety of new compounds. Safety profiles of various synthesized compounds were predicted using this tool. The data provided in Table 3 revealed that bicyclogermacrene presented carcinogenic potential and that β-selinene did not present carcinogenic potential in mice, but in rats it was positive. Regarding mutagenicity, the *in silico* evaluation is performed using the Ames test, which uses strains of the bacterium *Salmonella typhimurium* (TA100_10RLI; TA100_NA; TA1535_10RLI; TA1535_NA). The Ames toxicity test was used to identify whether a compound is mutagenic or not, that is, this test with the strains identifies agents that can cause mutagenic changes, they can be evaluated in the presence or absence of the S9 fraction, and this fraction evaluates the metabolism substances, being composed of microsomal and cytosolic hepatic fractions, simulating the characteristics of synthesized metabolites.[69] The TA100 strain demonstrates the ability of the substance to cause genetic coding substitutions in the guanine-cytosine pair, on the other hand, the TA1535 strain detects substances that can cause methylation induction and guanine-cytosine

base pair replacement.[70] That said, it was possible to verify that β-selinene was predicted as a mutagen while bicyclogermacrene was not. However, for the other lineages, both were not considered.[60,71]

To verify the possible cardiotoxicity, the hERG (human ether-related gene) parameter is analyzed, which indicates that both compounds present medium risk. According to Elmaidomy *et al*.,[63] hERG is a gene that encodes a protein known as Kv 11.1, the α subunit of a potassium ion channel. This ion channel is best known for its contribution to the electrical activity of the heart. The hERG channel mediates the repolarizing current IKr in the cardiac action potential, which helps coordinate heartbeats.[72] Correlating with the results, the average risk for hERG inhibition indicated that the engineered derivatives have an average risk in cardiac action potential, which thus indicates a need for more care when related to the individual who has cardiovascular problems.[68]

Therefore, there is a need to carry out toxicological studies to determine safety parameters that are not observed during the popular use of medicinal plant derivatives, thus constituting a very relevant analysis, since the effects of the compounds produced and simulated from their administration are characterized, helping to decide whether these compounds should be adopted for clinical use.[73]

Another parameter analyzed was drug-likeness, which qualitatively evaluates the chance of a molecule, that is, of the compounds β-selinene and bicyclogermacrene, to become an oral drug due to its bioavailability. SwissADME[26] provides access to five different rule-based filters, with different ranges of properties within which the molecule is defined as a drug. These filters often originate from analyses by large pharmaceutical companies to improve the quality of their proprietary chemical collections. The Lipinski method is widely used, and both compounds showed only 1 violation, still being considered adequate. The Ghose (Amgen), Veber (GSK), Egan (Pharmacy), and Muegge (Bayer) methods were adopted. Various estimates allow for consensus views or the choice of methods that best fit the specific needs of the end user in terms of chemical space or project-related demands. Any violation of any rule described here appears explicitly in the output pane. Among these three Ghose (Amgen), Veber (GSK), and Egan (Pharmacy) both compounds did not show any violation. For the Muegge (Bayer) method, β-selinene presented two violations, being considered inadequate, and bicyclogermacrene only one.

The bioavailability score is similar but seeks to predict the probability of a compound having at least 10% oral bioavailability in rats or measurable Caco-2 permeability, in general, this score needs to be at least 0.10 for the compound to be a candidate and, according to the data described in Table 3, both are considered candidates to be a drug with oral administration.[73] Another important analysis is related to the substructures of certain molecules that can present a potent response, regardless of the molecular target, this is called promiscuous compounds (PAINS). According to Baell *et al*.,[74] these substructures can present undue biological results, SwissADME returns to the possibility of such substructures existing and according to Table 3, neither β-selinene nor bicyclogermacrene presents the formation of these substructures. In addition to this verification, the Brenk analysis is associated with verifying whether these substructures are potentially toxic, reactive, metabolically unstable, or present weak pharmacokinetic characteristics, according to the analyses, there was only one fragment with such characteristics associated with the lead likeness criteria that is similar to drug-likeness but with a physicochemical approach that identifies it as a suitable molecule for a probable optimization, which may be involved to size and lipophilicity.[27] In this case, two violations were found for both molecules, indicating that there is a possibility that they suffer adjustments related to size and lipophilicity and consequent improvement in their biodistribution.

In the end, a synthetic accessibility score is provided related to the possibility of synthesis of such molecules evaluated in this study, verifying their ease.[27] The score ranges from 1 to 10, where 1 is said to be effortless to synthesize and 10 is said to be very difficult to synthesize. According to Table 3, the β-selinene compound presented a score of 3.42, while bicyclogermacrene presented a score of 4.34, both classified as having moderate ease of synthesis. It is noteworthy that this molecular scoring is complex and considers the presence of non-standard structural features, such as large rings, non-standard ring fusions, stereo complexity, and molecule size.[75]

Conclusions

Due to the great damage caused by the SARS-CoV-2 pandemic in 2020, the search for treatment or antiviral substances is constant. The number of mutations that this virus is capable of carrying out and causing the number of cases to rise in some regions is still a global concern. In this context, this article wanted to evaluate the antiviral potential of the species *Commiphora leptophloeos*, for this, its essential oil was obtained and its chemical characterization by GC-MS allowed us to identify nine terpenes and through molecular docking with the Mpro protein and chimeric SARS-CoV-2 receptor complexed with its human ACE2 receptor we could understand their

interactions, after molecular docking, two compounds showed promise in interacting with these important molecular targets for the interaction and internalization of the virus in the cells of its hosts. The compounds bicyclogermacrene and β-selinene had the highest scores and were then analyzed for pharmacokinetics, toxicity, and drug-likeness, also showing promising results with scores within the standards of drugs already used in the market. The use of bioinformatics tools helped us to filter out the compounds with the greatest potential and could help in future work about the stages of obtaining the essential oil and even in the possible isolation of such molecules so that *in vitro* tests can be conducted.

Supplementary Information

Supplementary data (compounds table, chromatogram, mass spectrum, and figures of interactions between compounds and M protein or spike) are available free of charge at http://jbcs.sbq.org.br as PDF file.

Acknowledgments

The authors are grateful to Coordenação de Aperfeiçoamento de Pessoal de Nível Superior - PNPD/CAPES (process numbers: 88887.357888/2019-00 and 88887.476154/2020-00).

Author Contributions

Michel R. R. Souza was responsible for conceptualization, data curation, formal analysis, investigation, methodology, validation, visualization, writing (original draft, review and editing); Daniela Droppa-Almeida for conceptualization, data curation, formal analysis, investigation, methodology, validation, visualization, writing (original draft, review and editing); Helena A. C. Kodel for formal analysis, methodology, validation, writing (original draft, review and editing); Tatiane B. Santos data for methodology, writing (review and editing); Ashlley S. Moraes for methodology; Laiza C. Krause for supervision; Thiago R. Bjerk for project administration, supervision, validation, visualization, writing (review and editing).

References

1. World Health Organization; *WHO Coronavirus (COVID-19) Dashboard*, https://covid19.who.int/table, accessed in July 2024.
2. Chtita, S.; Belaidi, S.; Qais, F. A.; Ouassaf, M.; AlMogren, M. M.; Al-Zahrani, A. A.; Bakhouch, M.; Belhassan, A.; Zaki, H.; Bouachrine, M., Lakhlifi, T.; *J. King Saud Univ., Sci.* **2022**, *34*, 102226. [Crossref]
3. Belhassan, A.; Chtita, S.; Zaki, H.; Alaqarbeh, M.; Alsakhen, N.; Almohtaseb, F.; Lakhlifia, T.; Bouachrine, M.; *J. Mol. Struct.* **2022**, *1258*, 132652. [Crossref]
4. Lima, N. M.; Andrade, T. J. A. S.; Acquah, K. S.; Oliveira, M. A. L.; Gois, K. F.; Medeiros, L. C. M.; *Quim. Nova* **2021**, *44*, 667. [Crossref]
5. Ouassaf, M.; Belaidi, S.; Mogren, M. M. A.; Chtita, S.; Khan, S. U.; Htar, T. T.; *J. King Saud Univ., Sci.* **2021**, *33*, 101352. [Crossref]
6. Belhassan, A.; Zaki, H.; Chtita, S.; Alaqarbeh, M.; Alsakhen, N.; Benlyas, M.; Lakhlifi, T.; Bouachrine, M.; *Comput. Biol. Med.* **2021**, *36*, 104758. [Crossref]
7. Dantas-Medeiros, R.; Marena, G. D.; Araújo, V. H. S.; Bezerra Neto, F. A.; Zanatta, A. C.; Lopes, N. P.; Bermejo, P.; Guerra, J. A.; Bedoya, L. M.; Fonseca-Santos, B.; Amorim-Carmo, B.; Fernandes-Pedrosa, M. F.; Chaves, G. M.; Bauab, T. M.; Chorilli, M.; Zucolotto, S. M.; *J. Drug Delivery Sci. Technol.* **2023**, *85*, 104531. [Crossref]
8. Dantas-Medeiros, R.; Furtado, A. A.; Zanatta, A. C.; Torres-Rêgo, M.; Lourenço, J. S. F.; Alves, E. M. G.; Galinari, E.; Rocha, H. A. O.; Guerra, G. C. B.; Vilegas, W.; Araújo, T. A. S.; Fernandes-Pedrosa, M. F.; Zucolotto, S. M.; *J. Ethnopharmacol.* **2021**, *264*, 113229. [Crossref]
9. Souza, M. R. R.; Santos, E.; Moraes, A. S.; Ribeiro, I. C. S.; Pinto, K. B.; Caramão, E. B.; Bjerk, T. R.; Krause, L. C.; *Sustainable Chem. Pharm.* **2023**, *33*, 101128. [Crossref]
10. Pessoa, R. F.; Figueiredo, I. A. D.; Ferreira, S. R. D.; Silva, A. R. L. F. C.; Paiva, R. L. M.; Cordeiro, L. V.; Lima, E. O.; Cabrera, S. P.; Silva, T. M. S.; Cavalcante, F. A.; *J. Ethnopharmacol.* **2021**, *268*, 113564. [Crossref]
11. Agra, M. F.; Baracho, G. S.; Nurit, K.; Basílio, I. J. L. D.; Coelho, V. P. M. J.; *J. Ethnopharmacol.* **2007**, *111*, 383. [Crossref]
12. Cartaxo, S. L.; Souza, M. M. A.; Albuquerque, U. P. J.; *J. Ethnopharmacol.* **2010**, *131*, 326. [Crossref]
13. Silva, R. C. S.; Milet-Pinheiro, P.; Silva, P. P. C. B.; Silva, A. G.; Vanusa, M.; *Plos One* **2015**, *10*, e0144586. [Crossref]
14. Pinto, K. B.; dos Santos, P. H. B.; Krause, L. C.; Caramão, E. B.; Bjerk, T. R.; *Braz. J. Pharm. Sci.* **2022**, *58*, e21609. [Crossref]
15. Lima, C. S.; Santos, H. R. S.; Albuquerque, U. P.; Silva, F. S. B.; *Ind. Crops Prod.* **2017**, *104*, 28. [Crossref]
16. Silva, I. F.; Guimarães, A. L.; Amorim, V. S.; Silva, T. M. G.; Peixoto, R. M.; Nunes, X. P.; Silva, T. M. S.; Costa, M. M.; *Cienc. Anim. Bras.* **2019**, *20*, e57228. [Crossref]
17. Loera, D. In *Biomedical Innovations to Combat COVID-19*; Rosales-Mendonza, S.; Comas-Garcia, M.; Gonzales-Ortega, O., eds.; Academic Press: New York, 2021, ch. 18. [Crossref]
18. Reddy, B. U.; Routhu, N. K.; Kumar, A.; *Microb. Pathog.* **2022**, *168*, 105512. [Crossref]

19. Dool, H. V. D.; Kratz, P. D. J.; *J. Chromatogr. A* **1963**, *11*, 463. [Crossref]
20. Adams, R. P.; *Identification of Essential Oil Components by Gas Ghromatography/Mass Spectrometry*, 4th ed.; Allured: Carol Stream, USA, 2017.
21. PubChem, https://pubchem.ncbi.nlm.nih.gov, accessed in July 2024.
22. Protein Data Bank (PDB), https://www.rcsb.org, accessed in July 2024.
23. Trott, O.; Olson, A. J.; *J. Comput. Chem.* **2010**, *31*, 455. [Crossref]
24. *Biovia*, *Discovery Studio Visualizer*, v. 4.5; Dassault Systèmes, San Diego, USA, 2022.
25. Guedes, I. A.; da Silva, M. M. P. P.; Galheigo, M.; Krempser, E.; de Magalhães, C. S.; Correa Barbosa, H. J.; Dardenne, L. E.; *J. Mol. Biol.* **2024**, 168548. [Crossref]
26. Daina, A.; Michielin, O.; Zoete, V.; *Sci. Rep.* **2017**, *7*, 42717. [Crossref]
27. *PreADMET and Prediction of ADME/Tox*, version 2.0; Bioinformatics and Molecular Design Research Center, South Corea, 2004.
28. Shen, T.; Li, G. H.; Wang, X. N.; Lou, H. X.; *J. Ethnopharmacol.* **2012**, *142*, 319. [Crossref]
29. Shimada, T.; Endo, T.; Rodríguez, A. A.; Fujii, H.; Nakano, M.; Sugiyama, A.; Shimizu, T.; Peña, L.; Omura, M.; *Sci. Hortic.* **2012**, *145*, 102. [Crossref]
30. Carvalho, C. E. S.; Sobrinho-Junior, E. P. C.; Brito, L. M.; Nicolau, L. A. D.; Carvalho, T. P.; Moura, A. K. S.; Rodrigues, K. A. F.; Carneiro, S. M. P.; Arcanjo, D. D. R.; Citó, A. M. G. L.; Carvalho, F. A. A.; *Exp. Parasitol.* **2017**, *175*, 59. [Crossref]
31. PubMEd, https://pubmed.ncbi.nlm.nih.gov, accessed in July 2024.
32. Zhang, X. Y.; Zhou, Y.; Wei, Z. P.; Shen, J.; Wang, L. K.; Ma, Z. Q.; Zhang, X.; *Pest Manage. Sci.* **2018**, *74*, 1630. [Crossref]
33. Farag, R. S.; Shalaby, A. S.; El-Baroty, G. A.; Ibrahim, N. A.; Ali, M. A.; Hassan, E. M.; *Phytother. Res.* **2004**, *18*, 30. [Crossref]
34. Joycharat, N.; Greger, H.; Hofer, O.; Saifah, E.; *Phytochem.* **2008**, *69*, 206. [Crossref]
35. Feng, J.; Bai, X.; Cui, T.; Zhou, H.; Chen, Y.; Xie, J.; Shi, Q.; Wang, H.; Zhang, G.; *Curr. Microbiol.* **2016**, *73*, 317. [Crossref]
36. He, W.; Zhai, X.; Su, J.; Ye, R.; Zheng, Y.; Su, S.; *Pathogens* **2019**, *8*, 258. [Crossref]
37. Liao, Q.; Qian, Z.; Liu, R.; An, L.; Chen, X.; *Antiviral Res.* **2013**, *100*, 578. [Crossref]
38. Chen, Y.; Dong, Y.; Jiao, Y.; Hou, L.; Shi, Y.; Gu, T.; *Arch. Virol.* **2015**, *160*, 1415. [Crossref]
39. Li, L.; Xie, Q.; Bian, G.; Zhang, B.; Wang, M.; Wang, Y.; Chen, Z.; Li, Y.; *Fitoterapia* **2020**, *142*, 104489. [Crossref]
40. Wu, H.; Liu, Y.; Zu, S.; Sun, X.; Liu, C.; Liu, D.; Zhang, X.; Tian, J.; Qu, L.; *Arch. Virol.* **2016**, *161*, 1559. [Crossref]
41. Hassanin, O.; Abdallah, F.; Galal, A. A.; *Comp. Immunol., Microbiol. Infect. Dis.* **2020**, *73*, 101547. [Crossref]
42. Venturi, C. R.; Danielli, L. J.; Klein, F.; Apel, M. A.; Montanha, J. A.; Bordignon, S. A. L.; Roehe, P. M.; Fuentefria, A. M.; Henriques, A. T.; *Pharm. Biol.* **2015**, *53*, 682. [Crossref]
43. Schnitzler, P.; Astani, A.; Reichling, J.; *J. Evidence-Based Complementary Altern. Med.* **2011**, *2011*, 253643. [Crossref]
44. Chatow, L.; Nudel, A.; Nesher, I.; Hemo, D. H.; Rozenberg, P.; Voropaev, H.; Winkler, I.; Levy, R.; Kerem, Z.; Yaniv, Z.; Eyal, N.; *Life* **2021**, *11*, 290. [Crossref]
45. Jha, N. K.; Sharma, C.; Hashiesh, H. M.; Arunachalam, S.; Meeran, M. N.; Javed, H.; Patil, C. R.; Goyal, S. N.; Ojha, S.; *Front. Pharmacol.* **2021**, *12*, 590201. [Crossref]
46. Dunkić, V.; Vuko, E.; Bezić, N.; Kremer, D.; Ruščić, M.; *Chem. Biodiversity* **2013**, *10*, 1894. [Crossref]
47. Chiang, L. C.; Ng, L. T.; Cheng, P. W.; Chiang, W.; Lin, C. C.; *Clin. Exp. Pharmacol. Physiol.* **2005**, *32*, 811. [Crossref]
48. Najar, B.; Mecacci, G.; Nardi, V.; Cervelli, C.; Nardoni, S.; Mancianti, F.; Ebani, V. V.; Giannecchini, S.; Pistelli, L.; *Molecules* **2021**, *26*, 2826. [Crossref]
49. Torky, Z. A.; Moussa, A. Y.; Abdelghffar, E. A.; Abdel-Hameed, U. K.; Eldahshan, O. A.; *Food Funct.* **2021**, *12*, 4630. [Crossref]
50. Loizzo, M. R.; Saab, A.; Tundis, R.; Statti, G. A.; Lampronti, I.; Menichini, F.; Gambari, R.; Cinatl, J.; Doerr, H. W.; *Phytomedicine* **2008**, *15*, 79. [Crossref]
51. Torres, P. H. M.; Sodero, A. C. R.; Jofily, P. F. P.; Silva-Junior.; *Int. J. Mol Sci.* **2019**, *20*, 4574. [Crossref]
52. Ferreira, L. G.; dos Santos, R. N.; Oliva, G.; Andricopulo, A. D.; *Molecules* **2015**, *20*, 13384. [Crossref]
53. Shityakov, S.; Broscheit, J.; Roewer, N.; Förster, C.; *Mol. Immunol.* **2013**, *56*, 305. [Crossref]
54. Jarunglumlert, T.; Nakagawa, K.; Adachi, S.; *Food Struct.* **2015**, *5*, 42. [Crossref]
55. Sharma, V.; Anandhakumar, S.; Sasidharan, M.; *Mater. Sci. Eng., C* **2015**, *56*, 39. [Crossref]
56. Lipinski, C. A.; Lombardo, F.; Dominy, B. W.; Feeney, P. J.; *Adv. Drug Delivery Rev.* **2001**, *46*, 3. [Crossref]
57. Veber, D. F.; Johnson, S. R.; Cheng, H. Y.; Smith, B. R.; Ward, K. W.; Kopple, K. D.; *J. Med. Chem.* **2002**, *45*, 2615. [Crossref]
58. Ntie-Kang, F.; Lifongo, L. L.; Mbah, J. A.; Owono L. C.; Megnassan, E.; Mbaze, L. M.; Judson, P. N.; Sippl, W.; Efange, S. M. N.; *In Silico Pharmacol.* **2013**, *1*, 12. [Crossref]
59. Yalçın, S.; Yalçınkaya, S.; Ercan, F.; *J. Mol. Struct.* **2021**, *1240*, 130556. [Crossref]
60. Moura, M. C. L.; Araújo, V. L. L.; Sousa, J. A.; *Res. Soc. Dev.* **2020**, *9*, e170932242. [Crossref]
61. Cho, C. F.; Wolfe, J. M.; Fadzen, C. M.; Calligaris, D.; Hornburg, K.; Chiocca, E. A.; Agar, N. Y. R.; Pentelute, B. L.; Lawler, S. E.; *Nat. Commun.* **2017**, *8*, 15623. [Crossref]
62. Dolabela, M. F.; Silva, A. R. P.; Ohashi, L. H.; Bastos, M. L. C.; Silva, M. C. M.; Vale, V. V.; *Rev. Fitos* **2018**, *12*, 227. [Crossref]

63. Elmaidomy, A. H.; Alhadrami, H. A.; Amin, E.; Aly, H. F.; Othman, A. M.; Rateb, M. E.; Hetta, M. H.; Abdelmohsen, U. R.; Hassan, H. M.; *Molecules* **2020**, *25*, 3116. [Crossref]
64. Nisha, C. M.; Kumar, A.; Vimal, A.; Bai, B. M.; Pal, D.; Kumar, A.; *J. Mol. Graphics Modell.* **2016**, *65*, 100. [Crossref]
65. Kovačević, S. Z.; Jevrić, L. R.; Kuzmanović, S. O. P.; Lončar, E. S.; *Iran. J. Pharm. Res.* **2014**, *13*, 899. [Link] accessed in July 2024
66. dos Santos, R. C.; Daniel, I. C.; Próspero, D. F. A.; da Costa, C. L. S.; *Bol. Inf. Geum* **2018**, *9*, 31. [Link] accessed in July 2024
67. Dewanjee, S.; Dua, T. K.; Bhattacharjee, N.; Das, A.; Gangopadhyay, M.; Khanra, R.; Joardar, S.; Riaz, M.; Feo, V. D.; Zia-Ul-Haq, M.; *Molecules* **2017**, *22*, 871. [Crossref]
68. Santana, L. E. G. S.; Miranda, I. K. I.; Sousa, J. A.; *Res. Soc. Dev.* **2020**, *9*, 81991110469. [Crossref]
69. Claxton, L. D.; Umbuzeiro, G. A.; DeMarini, D. M.; *Environ. Health Perspect.* **2010**, *118*, 1515. [Crossref]
70. de Grandis, R. A.; Resende, F. A.; da Silva, M. M.; Pavan, F. R.; Batista, A. A.; Varanda, E. A.; *Mutat. Res.* **2016**, *798-799*, 11. [Crossref]
71. Fowler, K.; Fields, W.; Hargreaves, V.; Reeve, L.; Bombick, B.; *Toxicol. Rep.* **2018**, *5*, 542. [Crossref]
72. Cherubini, A.; Hofmann, G.; Pillozzi, S.; Guasti, L.; Crociani, O.; Cilia, E.; Stefano, P. D.; Degani, S.; Balzi, M.; Olivotto, M.; Wanke, E.; Becchetti, A.; Defilippi, P.; Wymore, R.; Arcangeli, A.; *Mol. Biol. Cell* **2005**, *16*, 2972. [Crossref]
73. de Lima-Saraiva, S. R. G.; Guimarães, A. L.; de Oliveira, A. P.; Saraiva, H. C. C.; de Oliveira-Junior, R. G.; de Barros, V. R. P.; Menezes, V. G.; de Oliveira, R. A.; Silva, F. S.; de Lima, R. S.; *Afr. J. Biotechnol.* **2012**, *11*, 13998. [Crossref]
74. Baell, J. B.; Holloway, G. A.; *J. Med. Chem.* **2010**, *53*, 2719. [Crossref]
75. Ertl, P.; Schuffenhauer, A.; *J. Cheminf.* **2009**, *1*, 8. [Crossref]

Submitted: November 6, 2023
Published online: July 29, 2024